ACS APPLIED MATERIALS & INTERFACES

Research Article

www.acsami.org

Aesthetically Pleasing Conjugated Polymer:Fullerene Blends for Blue-Green Solar Cells Via Roll-to-Roll Processing

Chad M. Amb,[†] Michael R. Craig,[†] Unsal Koldemir,[†] Jegadesan Subbiah,[‡] Kaushik Roy Choudhury,[‡] Suren A. Gevorgyan,[§] Mikkel Jørgensen,[§] Frederik C. Krebs,*[,§] Franky So,*[,‡] and John R. Reynolds*[,†]

[§]Department of Energy Conversion and Storage, Technical University of Denmark, Frederiksborgvej 399, DK-4000 Roskilde, Denmark

[‡]Department of Materials Science and Engineering and The George and Josephine Butler Polymer Research Laboratory, [†]Department of Chemistry, Center for Macromolecular Science and Engineering, University of Florida, Box 117200, Gainesville, Florida 32611, United States

ABSTRACT: The practical application of organic photovoltaic (OPV) cells requires high throughput printing techniques in order to attain cells with an area large enough to provide useful amounts of power. However, in the laboratory screening of new materials for OPVs, spin-coating is used almost exclusively as a thin-film deposition technique due its convenience. We report on the significant differences between the spin-coating of laboratory solar cells and slot-die coating of a blue-green colored, low bandgap polymer (PGREEN). This is one of the first demonstrations of slot-die-coated polymer solar cells OPVs not utilizing poly(3-hexylthiophene):(6,6)-phenyl-C_{61}-butyric acid methyl ester (PCBM) blends as a light absorbing layer. Through synthetic optimization, we show that strict protocols are necessary to yield polymers which achieve consistent photovoltaic behavior. We fabricated spin-coated laboratory scale OPV devices with PGREEN: PCBM blends as active light absorbing layers, and compare performance to slot die-coated individual solar cells, and slot-die-coated solar modules consisting of many cells connected in series. We find that the optimum ratio of polymer to PCBM varies significantly when changing from spin-coating of thinner active layer films to slot-die coating, which requires somewhat thicker films. We also demonstrate the detrimental impacts on power conversion efficiency of high series resistance imparted by large electrodes, illustrating the need for higher conductivity contacts, transparent electrodes, and high mobility active layer materials for large-area solar cell modules.

KEYWORDS: *polymer solar cells, roll-to-roll printing/coating, slot-die coating, low band gap polymers*

INTRODUCTION

Conjugated polymers are promising light-harvesting materials in photovoltaic devices as they are expected to reduce processing costs through the use of roll-to-roll processing techniques. Additionally, the ability for organic photovoltaic devices (OPVs) to be flexible and to control the color of the materials[1] opens the doors to new markets that may not be applicable to their inorganic counterparts. Significant efforts have been undertaken to develop new materials and understand structure−function relationships in laboratory cells prepared by spin-coating, but few studies have utilized high throughput printing techniques to produce useful prototypes with these new materials. Although roll-to-roll processing of organic solar cells is critical to them reaching the marketplace, because of the convenience of spin-coating, almost all of the device fabrication in academic research concerning the development of new materials is done using this method as a processing technique. Additionally, most reports that utilize high-throughput printing techniques use poly(3-hexylthiophene) (P3HT) as the light-harvesting material.[2−5] To date, there have been few reports where other materials have been used as active layers in organic solar cells where the processing is carried out with a method applicable to roll-to-roll coating. Herein, we investigate the transition from laboratory bulk heterojunction solar cells prepared by spin-coating to slot-die-coated prototype solar cells utilizing a blue-green-colored, low-bandgap conjugated polymer as the light harvesting material.

In the early days of bulk heterojunction solar cells, spin-coated active layers consisting of polymer/fullerene blends initially achieved power conversion efficiencies (PCE's) of ∼1% in 1995 using poly(phenylene-vinylene) (PPV) derivatives,[6] but device performance was limited by the low charge mobility and high bandgap of the PPV based materials.[7] In 2002, P3HT was found to be an effective OPV material[8] and recent efforts using P3HT have reported PCEs as high as 6.5%.[9] As P3HT does not absorb red light where the highest intensity of solar photons are emitted, efforts have been made to extend the absorption of

Received: January 27, 2012
Accepted: February 2, 2012
Published: February 21, 2012

dx.doi.org/10.1021/am300156p | ACS Appl. Mater. Interfaces 2012, 4, 1847−1853

active layer materials into the red region of the spectrum to make use of this energy.

The donor−acceptor (D−A) approach, alternating electron-rich and electron-poor heterocycles in a conjugated material, has led to soluble conjugated polymers which can absorb energies as low as 0.5 eV[10] and thus can be utilized to absorb a high proportion of solar radiation. This approach allows tuning of HOMO−LUMO levels of the polymers to be ideal in bulk heterojunction cells and allows the colors displayed by these systems to be controlled to a high degree. The D−A approach has resulted in BHJ solar cells displaying PCE's of up to 7.4%.[11,12]

A popular acceptor heterocycle used in OPVs is benzothiadiazole (BTD), where the BTD's low (but not too low) LUMO level has allowed donor−acceptor polymers to display long-wavelength absorption. Additionally, BTD has an appropriate LUMO energy level alignment with PCBM as PCE's in solar cells has exceeded 5% based on BTD containing materials.[13,14] Especially effective systems have employed fused thiophene derivatives alternating with BTD, as a number of groups has reported PCE greater than 5% with these systems.[15−18]

In BTD containing D−A polymers, it has recently been shown that the wavelength and intensity of the two bands of absorption can be controlled through modification of the donor-to-acceptor ratio in the polymer.[19] In these systems, the high energy band in a strictly alternating copolymer can be shifted entirely into the UV yielding a blue colored material,[20] and upon addition of higher contents of donor moiety or alkene linkages, the high energy band shifts into the visible, causing green hues to become apparent.[21] This approach has been used to give green colored polymers, some of which have been utilized in solar applications.[22] One such polymer has been PGREEN having the repeat unit structure shown in Figure 1.[23,24] Laboratory cells utilizing PGREEN have shown

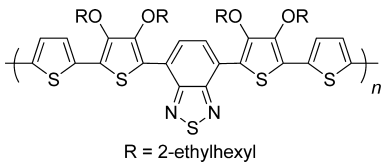

Figure 1. Repeat unit structure of PGREEN.

2% PCE when mixed with 6,6-phenyl-C_{61}-butyric acid methyl ester PCBM, giving green cells, and up to 2.7% when mixed with $PC_{71}BM$, to give red/brown colored cells. These colors are important as appearance could be the factor which determines whether or not sufficient demand for a certain product will exist. One such example of the necessity of green colored light harvesting materials are photovoltaics meant to emulate grass or other plants.[25]It should be noted that the electrochemical and photophysical properties of PGREEN have been documented in our previous reports.[23,24]

Along with the investigation of new materials, various methods for developing bulk heterojunction device architectures have been the subject of significant research.[26−29] Cells with a traditional architecture, where a transparent electrode (most commonly PEDOT:PSS-coated ITO) acts as a hole collecting anode, and a low work function metal (such as aluminum) acts as an electron harvesting cathode have been the standard for a number of years. More recently, "inverted" device architectures where holes migrate to the metal electrode, and electrons toward the transparent electrode have become more common, for a number of reasons. One advantage of the inverted cell geometry lies in the fact that the metal electrodes employed (generally Ag) are significantly more stable to ambient air when compared to the more active metals Al and Ca.[30,31] Another advantage is that the printing of high-work-function silver pastes is more suited to large-scale manufacture of cells as opposed to evaporation of Al and Ca, and the high activity of these metals makes creating printable pastes more challenging. Roll-to-roll printing of OPVs has generally been achieved using the inverted architecture.

When utilizing the device architectures described above, the vision of large-area polymer cells processed at great speed requires film forming techniques other than spin-coating. Many printing and coating techniques are available and some of them have been tested in the context of polymer solar cells.[32] Of those, roll-to-roll slot-die coating and screen printing have proven particularly adaptable and have enabled upscaling and large scale manufacture with little expensive active materials loss.[32,33] This has led to the development of complete processes and procedures for product integration[34] and demonstration.[35] From the development of new materials, to the successful integration into an application, there is a considerable effort that is often overlooked. The work reported here also describes the effort needed on that path from new material to demonstration in the form of a prototype.

In this contribution, we detail an optimized synthesis of PGREEN, wherein three oxidative polymerizations were carried out in order to determine synthetic procedures which give high molecular weight, high yielding and soluble polymers. The differences in three batches of material demonstrate the need for strict synthetic protocols to achieve consistent photovoltaic behavior. Laboratory-scale spin-coated bulk heterojunction devices were fabricated in both normal and inverted device structures, which showed optimized performance of ∼2% PCE when using inverted device architectures. A high throughput printing technique then allowed the fast screening of optimal polymer:PCBM ratio in printed cells, which was found to be quite different from the optimal ratio found for cells produced by spin-coating. Finally, large area blue-green colored solar cell prototypes made by slot-die coating were produced that achieved power conversion efficiencies near 0.3% for the printed modules. Differences between spin-coated cells and the printed modules demonstrate the importance of the resistance of the cells, which leads to significant decreases in the performance of large area cells, especially when multiple cells are connected in series.[36,37]

2. MATERIALS AND METHODS

Materials. All reagents and starting materials were purchased from commercial sources and used without further purification, unless otherwise noted. The synthesis of compound **M1** has been described previously.[23] The chloroform utilized as polymerization solvent was HPLC grade stabilized with 50 ppm pentene.

Preparation of $FeCl_3$ Solution. A solution of iron(III) chloride (bottle had never been opened, material was black solid) in nitromethane (ACS grade) was produced by dissolving $FeCl_3$ (4.5 g, 27.7 mmol) in 25 mL of nitromethane in a volumetric flask. Care was taken to quickly weigh the $FeCl_3$ and dissolve it to minimize absorption of atmospheric water, and the flask was capped as soon as the solvent was added.

Synthesis of PGREEN Batches PG1-PG3. Pentamer **M1** (1.00 g, 1.02 mmol) was transferred from a storage vial to a smaller vial by spatula. This was then rinsed into a 250 mL round-bottom flask with

chloroform (HPLC grade, stabilized with 50 ppm pentene), and then more chloroform was added so that the total volume of chloroform added was 170 mL. The flask was placed in a room temperature water bath which was maintained at a temperature of 18.8−19.9 °C throughout the experiment. Dry air was then bubbled into the solution through a stainless steel needle at a bubbling rate of about 2−3 bubbles per second. The reaction was then covered by aluminum foil to block ambient light, and was only removed periodically to check on the reaction. To this solution was added 4.6 mL of a 1.1 M solution of $FeCl_3$ in nitromethane via syringe pump. The pump was set at 2.3 mL/h at at a syringe diameter of 13 mm, and the addition took 2 h and 20 min to complete. The reaction was then stirred for 21 h and 40 min longer. After completion of the reaction, the mixture was poured into 500 mL methanol and stirred vigorously for 10 min. The reaction was then filtered on a course paper filter, and washed with 100 mL methanol. The methanol washings were then discarded, and a clean flask was placed under the filter. The paper was then punctured to allow solids to flow into the flask below, and the solids were washed down with ∼350 mL chloroform, yielding a dark suspension with a significant amount of soluble material. Hydrazine monohydrate (10 mL) was then added, and the mixture was stirred for 2 h at room temperature. The mixture was then concentrated to about 150 mL (rotary evaporation, room temp), and the mixture was pipetted into ∼350 mL of methanol. The resulting solid was filtered onto a cellulose thimble, and extracted (Soxhlet) with methanol (16 h), acetone (12 h), dichoromethane (12 h), and chloroform (until the extract was clear, ∼ 6 h). The chloroform soluble fraction was then cooled to room temperature, and 5 mL of hydrazine hydrate solution (80% in water) was added and stirred for 2 h. This fraction was then concentrated to 150 mL (by rotary evaporation, room temp), pipetted into 350 mL of methanol, and the resulting solid was filtered on a nylon filter membrane (GE magna, 20 μm pore size). The solid was then placed under vacuum (∼0.1 Torr) for 2 days to remove solvents to give 520 mg (52%) of a dark solid. (**PG1**) Elemental Anal. Calcd %: C, 66.49; H, 7.65; N, 2.87. Found: C, 66.33; H, 7.70; N, 2.83. ^{1}H NMR: 8.45 (bs, 2H), 7.34 (bs, 2H), 7.16 (bs, 2H), 4.05 (m, 8 H), 1.95 (bs, 2H), 1.8−1.0 (m, 34 H), 1.0−0.8 (m, 24 H). ^{1}H NMR spectra were not significantly different between batches **PG1**-**PG3**.

PG2 was synthesized using identical procedures as PG1, except that 0.3 mL of the iron(III) chloride solution was added over 2 min and the remainder added over 1.75 h, and the temperature maintained at 21.4−22.1 °C throughout. Yield 250 mg (25%). Elemental Anal. Found: C, 66.39; H, 7.96; N, 2.87.

PG3 was synthesized using identical procedures as **PG1**, except that the solid iron(III) chloride used was yellow in color (hydrated), and was dispersed in nitromethane, but not all of the 4.5 g used for the stock solution could be dissolved. Elemental Anal. Found: C, 66.44; H, 7.85; N, 2.81.

Characterization Methods. ^{1}H NMR spectra were collected on a Varian Inova 2 500 MHz instrument using $CDCl_3$ as a solvent and the residual $HCCl_3$ peak as references (^{1}H: δ = 7.26 ppm,). Elemental analyses were carried out by the CHN elemental analysis service in the Chemistry Department of the University of Florida. Gel permeation chromatography (GPC) was performed using a Waters Associates GPCV2000 liquid chromatography system with its internal differential refractive index detector (DRI) at 40 °C, using two Waters Styragel HR-5E columns (10 μm PD, 7.8 mm i.d., 300 mm length) with HPLC grade THF as the mobile phase at a flow rate of 1.0 mL/min. Injections were made at 0.05 - 0.07% w/v sample concentration using a 220.5 μL injection volume. Retention times were calibrated against narrow molecular weight polystyrene standards (Polymer Laboratories; Amherst, MA). UV−visible absorption spectroscopy was performed using a Varian Cary 500 UV−vis/NIR spectrophotometer.

Device Fabrication: 0.04 cm^2 Spin-Coated Cells. Bulk-heterojunction (BHJ) solar cells were fabricated by the spin-coating of 30-nm-thick layers of poly(3,4-ethylenedioxythiophene):poly-(styrenesulfonate) (PEDOT:PSS; Baytron AI 4083 from HC Starck) on ultrasonically cleaned and UV-ozone-treated, indium tin oxide (ITO)-coated, patterned glass substrates, followed by baking on a hot plate at 180 °C for 10 min. An active layer of the device consisting of the blend of polymer (PGREEN and PCBM (99% pure, Solenne BV) was then spin-coated from chlorobenzene solvent with a thickness of 120 nm. The device was subsequently heated on a hot plate at 70 °C for 30 min. LiF (1 nm) and aluminum (100 nm) were thermally evaporated at a vacuum of ∼1 × 10^{-7} mbar on top of active layer as a cathode (0.04 cm^2 active area).

For the inverted cells, a thin layer of sol−gel ZnO (35 nm) were spin-coated onto ITO-coated glass. The ZnO sol−gel films were then annealed in air for 30 min at 200 °C. The same process for the active layer in the conventional architecture was used for the inverted devices. After annealing the active layer, PEDOT:PSS (Baytron P diluted with isopropanol 3:1 V/V) was spin-coated onto the active layer to give a 35 nm film, and the film was annealed at 130 C for 5 min. Silver (80 nm) was then thermally evaporated on top of the PEDOT:PSS layer. The active area of the devices was 0.04 cm^2. The current density−voltage measurements of the devices were carried out using a 150 W Newport ozone free xenon arc lamp as the light source in conjunction with a Keithley 4200 semiconductor parameter analyzer system. Solar measurements were carried out under 1000 W/m^2 AM 1.5G illumination conditions. Device fabrication was carried out under nitrogen atmosphere and characterizations were performed in an ambient environment without any encapsulation.

Device Fabrication: 0.5 cm^2 Spin-Coated Cells. Glass substrates with precoated ITO layer (with sheet resistance of ∼12 Ω/□) patterned into four separate stripes were cleaned ultrasonically for 20 min in 2-propanol and then 20 min in demineralised water. In the case of inverted device structures, the demineralized water step is not required.

Normal geometry: An aqueous dispersion of PEDOT:PSS (1.3 wt % in H_2O as supplied from Aldrich) was deposited on glass/ITO by spin-coating at 2800 rpm followed by annealing of the substrates for 5 min at 150 °C. The active layer material was prepared by mixing PGREEN with PCBM at 1:8 ratio and dissolving the mixture in chlorobenzene by stirring at 50 °C for 1 day and finally filtering the solution through a 0.45 μm PVDF filter. The active layer was spin-coated at 600 rpm. Finally the samples were transferred into a vacuum evaporator and the Al electrode was evaporated on top of the devices.

Inverted geometry: A layer of ZnO nanoparticles dissolved in acetone at 45 mg/mL was coated on the glass/ITO at a spin speed of 1000 rpm followed by annealing of the films for 5 min at 120 °C. The same procedure was used for the active layer as described for the normal geometry devices. As a next step,a PEDOT:PSS (Agfa 5010) was coated on top of the active layer by first wetting the coating surface with 2-propanol and then spin-coating the PEDOT:PSS solution at 1000 rpm. The films were then annealed at 130 °C for 5 min. The layer of the PEDOT:PSS was made rather thick (a few μm) to ensure a good protection of the active layer from the back electrode silver paste diffusion. Finally, a silver paste was screen printed on the top of the devices and annealed for 2 min at 140 °C.

Slot-Die Coating. The general slot-die coating procedure followed our previous work.[33,34] Solutions of PGREEN and PCBM of respectively 30 mg/mL in chlorobenzene were employed for the ratio experiments, and a solution of 15 mg/mL in PGREEN and 15 mg/mL in PCBM was employed in the roll-to-roll manufacture of the modules. The coating speed of the active layer was 2 m/min and the wet thickness was 8 μm giving an approximate dry film thickness of 240 nm. The drying was carried out in a hot air oven at 140 °C. The rest of the processing following the descriptions found in the literature.[34]

Characterization. The devices were characterized using a KHS 575 solar simulator with the AM1.5G spectrum calibrated to 1 sun using a pyranometer. The devices were masked to ensure a correct illumination of the active area. The devices were placed under the simulator and IV characteristics were measured after the device temperature was stabilized (65 °C ± 3 °C).

3. RESULTS AND DISCUSSION

Synthesis. The synthesis of three batches of PGREEN was carried out as described in Scheme 1, with the intent of

Scheme 1. PGREEN Synthesis via $FeCl_3$ Induced Oxidative Polymerization

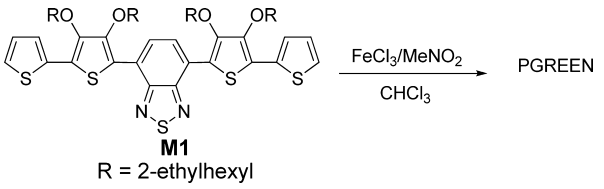

studying the effects of the rate of addition of the $FeCl_3$ oxidant, as well as the effects of using slightly hydrated $FeCl_3$ on polymer properties. Batch **PG1** was synthesized according to our previous work, where 5 equiv. of oxidant was added over 2 h using a syringe pump, and the yield and molecular weights were consistent with that previously reported.[23,24] It was found that a faster addition of $FeCl_3$ (**PG2**) (0.33 equiv. over 2 min, and the remainder over 1 h 45 min) resulted in a significantly lower yield and noticeably lower molecular weight of PGREEN as seen in Table 1, with a large amount of insoluble material

Table 1. Polymer Yield, Molecular Weight, and Spin-Coated Solar Cell Results for Three Batches of PGREEN[a]

polymer	yield (%)	M_n[b] (PDI)	V_{oc} (V)	I_{sc} (mA/cm^2)	FF	PCE (%)
PG1	52	57.3 (1.70)	0.75	5.16	45	1.73
PG2	25	37.3 (1.91)	0.77	4.56	37	1.28
PG3	58	28.2 (1.71)	0.79	5.14	47	1.90

[a]Solar cells fabricated using ITO/PEDOT:PSS/PGREEN:PCBM(1:8 ratio)/LiF/Al device architecture, with spin-coated PEDOT:PSS and active layer. [b]Number average molecular weight (kDa).

present after Soxhlet extraction. This result suggests that a significant amount of cross-linking through the unsubstituted thiophene moieties could have occurred. When using a slightly hydrated form of $FeCl_3$ (**PG3**), a further decrease in molecular weight occurred compared to **PG1** or **PG2**. This could be attributed to the lower reduction potential of hydrated $FeCl_3$ vs anhydrous $FeCl_3$ in $MeNO_2$,[38] thus giving a lower degree of polymerization. For all three polymers, CHN elemental analysis gave values within 0.4% of the theoretical value for the PGREEN repeat unit structure, suggesting little residual iron or other impurities were present in the samples.

Spin-Coated Solar Cells. The photovoltaic properties of spin-coated cells constructed using each of the polymer batches **PG1**-**PG3** were studied in donor−acceptor conventional architecture BHJ solar cells (Figure 2a) employing PCBM as the electron acceptor (polymer:PCBM blend ratio of 1:8.[23,24]) The illuminated J-V characteristics of the devices made with all three PGREEN polymers are shown in Figure 2c and the photovoltaic performances of the devices (**PG1**/**PG2**/**PG3**:PCBM) with conventional device structure is summarized in Table 1. Figure 2b also shows schematic diagrams of the inverted device architecture used to evaluate the photovoltaic performance of the polymers. In general, the performance characteristics for these cells are quite similar, indicating a useful reproducibility in our polymer preparations. As can be seen in Figure 2c, batch **PG3** displays the best overall performance with a power conversion efficiency (PCE) of 1.92%, whereas batch **PG2** shows the lowest performance with a PCE of 1.27%. From these results, it seems that the performance of the batches is independent of molecular weight over 28 kDa for this polymer, as no clear correlation between

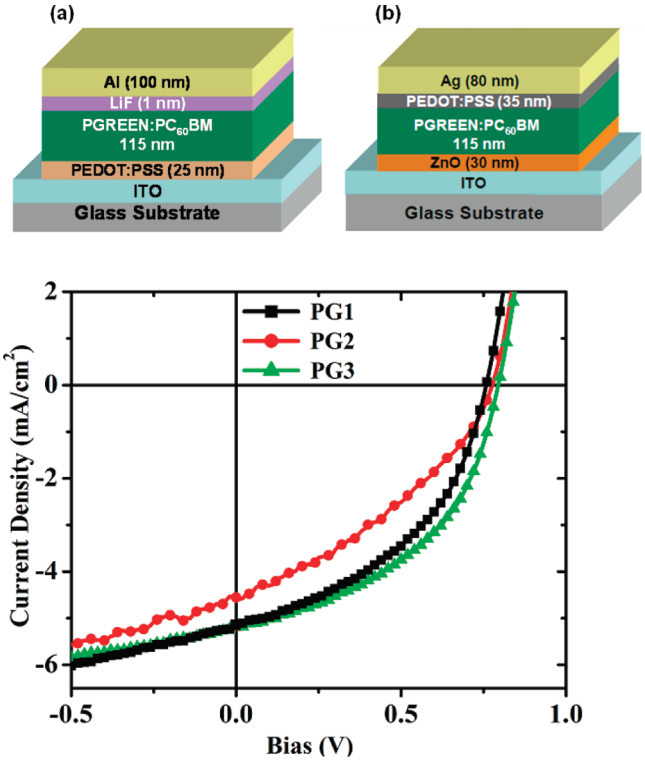

Figure 2. Schematic diagram of the PGREEN polymer solar cells with (a) conventional and (b) inverted geometry. (c) Current−voltage plots for illuminated conventional geometry cells (0.04 cm^2) for each of the three polymer batches produced under identical processing conditions.

molecular weight and performance exists in the series. In addition, the elemental analysis results of the three batches were near identical and were consistent with the calculated value for the polymer repeat unit, which makes differences in purity of the three batches unlikely as identical purification methods were used in all three cases. Using the oxidative polymerization methodology shown above, it is possible that the strong oxidant causes trace defects such as coupling through β positions and cross-linking, which could cause the differences in performance. The less oxidizing hydrated iron(III) chloride gave the best results as it likely did not cause as much defect formation. The cross-linking and β couplings would likely cause a change in morphology, which is known to cause differences in charge mobility through the polymer matrix.[39]

Batch **PG3** was then used in an inverted device (schematic shown in Figure 2b), and the illuminated current−voltage plots comparing the conventional and inverted architectures are shown in Figure 3. When utilizing the inverted cells, significant enhancements in PCE have been demonstrated based on favorable vertical phase morphology of the active layer.[40,41] This favorable morphology generally improves charge carrier collection and results in higher currents in the inverted cells. However, our inverted PV device exhibits a J_{sc} value of 5.67 mA/cm^2, a V_{oc} value of 0.78 V, a fill factor value of 45%, and PCE of 1.98%, which corresponds to only a 3% enhancement in PCE. Here, the likely reason for minimal enhancement of device performance for the inverted geometry is the high content (88%) of PCBM in the active layer, which can negate any favorable vertical phase morphology. Interestingly, when increasing device area in the conventional geometry, the short circuit current density decreased significantly from 5.14 to 3.64

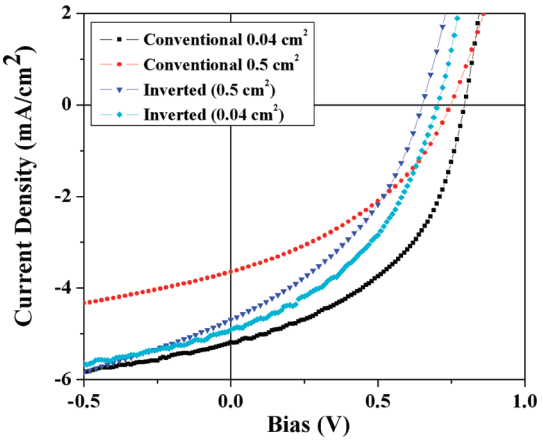

Figure 3. Illuminated current–voltage characteristics of solar cells made with **PG3** in conventional and inverted device geometries with 0.04 cm^2 or 0.5 cm^2 device area.

mA/cm^2, with PCE decreasing to 1.06% from 1.90% with the smaller area cell. The estimated series resistance also increased from ~35 to ~70 Ω cm^2, possibly attributable to this change in the geometrical area of the devices. In inverted devices where PEDOT:PSS was used as an interlayer between the active layer and silver, a smaller reduction in PCE was observed, from 1.46 to 1.18%, with small losses in fill factor and V_{oc}. A significant difference in series resistance between those cells was not observed, with a value of around 45 Ω cm^2 for each. Also, there was no difference between 0.04 cm^2 inverted cells using ZnO nanoparticles vs ZnO produced by sol–gel methods. It should be noted that cells using P3HT:PCBM as an active layer have been reported with series resistance of 1.6 Ω cm^2 using 0.06 cm^2 cells.[37] In that report, it was shown that series resistance values of greater than 10 Ω cm^2 cause significant reduction in fill factor and short circuit current. It can also be expected that the large resistance values will cause even more significant device performance losses when many cells are connected in series, as is shown in the following sections.

Slot-Die-Coated Solar Cells. The roll-to-roll preparation of solar cells based on the highest performing batch of PGREEN, **PG3**, by using slot-die-coated active layers and screen printed metal back electrodes followed two approaches. First, single cells were prepared by differentially pumped slot-die coating to enable identification of the optimum **PG3**:PCBM ratio. In this case, single-cell devices were prepared by altering the **PG3**:PCBM ratio along the length of the foil as described previously.[42] This experiment gives single solar cell devices and identifies that **PG3**:PCBM range that is optimal for roll to roll processing of modules It should be noted that one necessary difference in the processing of the cells are the temperatures required to remove the carrier solvent. In spin-coating, most of the solvent is removed during the spinning process, but in slot-die coating, the solvent must be removed in an oven, in this case at 140 °C. In spin-coated conventional architecture cells, a small decrease in PCE was observed after heating to 150 °C for 10 min, from 1.73 to 1.53%, showing a small but not overly detrimental degradation in performance after heating to such temperatures.

Figure 4a shows the PCE as a function of PCBM content of inverted architecture solar cells having an active area of 4.2 cm^2 processed by differentially pumped slot-die coating. This large active area is important to note, and quickly brings out the

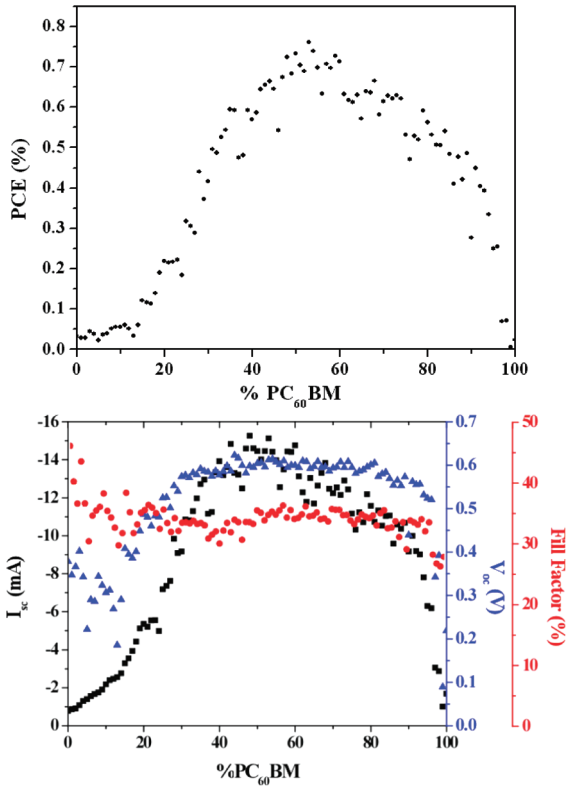

Figure 4. (a) PCE Optimization of **PG3**: PCBM ratio in steps of 1% using a fast roll to roll procedure.[42] The active area of the cells was 4.2 cm^2. (b) Short circuit current (I_{sc}), open circuit voltage (V_{oc}), and fill factor (%) as a function of the polymer:PCBM concentration in the slot-die printed cells.

utility of this processing method to potentially useful solar cells. Here, it can be seen that the maximum performance reached was between 0.7 to 0.8% PCE for devices with **PG3**:PCBM ratios in the range of 1:1. This is significantly different than the optimal ratio of 1:8 polymer:PCBM that was found for the spin-coated, conventional geometry laboratory cells. To further evaluate the causes for this behavior, Figure 4b shows the short circuit current (I_{sc}), open circuit voltage (V_{oc}), and fill factor (%) as a function of the polymer:PCBM concentration in the slot-die printed cells. It can be seen that the peak in PCE at around 50% PCBM content is driven by a maximum in short circuit current, as open circuit voltage is quite stable at around 0.6 V between 20 and 90% PCBM content. We believe that the significant difference in optimal polymer/fullerene ratio in the slot-die-coated cells vs the spin-coated cells is due differences in active layer thickness. Previously we found the optimal active layer thickness of 1:8 polymer:PCBM blends was 120 nm with spin-coating, but in slot-die coating device yield is significantly increased when greater film thickness is utilized;[44] therefore we chose to use thicker films to print modules (240 nm). Thicker active layer films are required to ensure mechanical robustness and defect free coatings,[43] and as well as increasing device yield.[44] Importantly, near quantitative device yield is critical since there are many cells connected in series. If a short or open circuit exists in one cell it could cause the entire module to fail. Thicker active layer films were also necessary to give the intended color intensity of the modules. However, using thicker films with such a low content of polymer probably resulted in less efficient collection of holes due to more "dead ends" in polymer domains. Also, previous studies have shown that

polymer-fullerene blend morphology is similar between spin-coated cells and slot-die-coated cells, given that the films are cast from the same solvent and concentration.[45] The fill factor remains a modest 30−35% across the full range of PCBM contents, lower than the spin-coated cells in this report as well as our previous reports studying this polymer.[23,24] Possible explanations for this are larger resistive losses in the large area devices on flexible substrates and the more poorly conducting electrodes, as well as again the increased thickness.

Fifty large modules measuring 25 × 25 and comprising 12 serially connected cells were then prepared by slot-die coating and screen printing. The total active area each of the modules, which only includes the area printed with **PG3**:PCBM, was 450 cm^2. As such, use of approximately 0.5 g of a sample PGREEN allowed the printing of 22,500 cm^2 (2.25 m^2) of active solar cell. A photograph of one of the modules is shown in Figure 5,

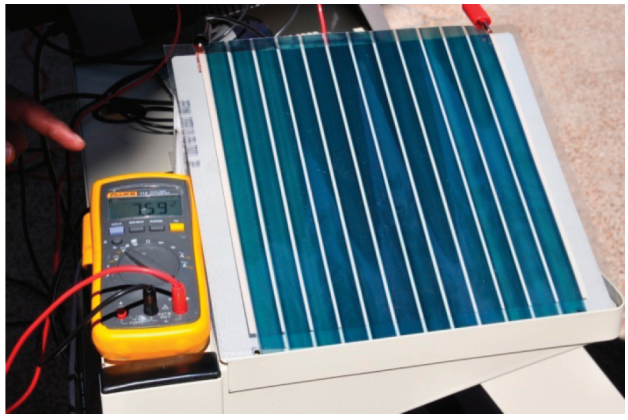

Figure 5. Photograph of a slot-die-coated, inverted architecture solar cell module. The photograph was taken on a bright sunny day in Florida.

where the module is illuminated on a sunny Florida day and an open circuit voltage of 7.59 V can be observed across the device.

The power conversion efficiency as a function of module number is shown in Figure 6a, and the I_{sc}, V_{oc}, and fill factor as a function of module number is shown in Figure 6b. As can be seen from Figure 6a, the PCE of the cells across the device was generally around 0.3%, except for modules 25−35, and modules 45−50. When printing modules, a run-in period is required for optimal alignment of layers (modules 1−10), followed by a period of production of actual prototypes, followed by a run-out period. As there is little room for error in alignment in the cells, any misalignment can have a detrimental impact on the PCE, which occurred in modules 30−35 and 45−50. The PCE loss from 0.7% for the printed 4 cm^2 to 0.3% for the printed modules can be attributed to the series connections of the modules, which further increased the resistance across the device to 37 000 Ω cm^2. Because of the higher series resistance values for PGREEN-based cells vs P3HT-based cells, it can be expected that a larger performance reduction would be experienced when large modules, where a number of cells are connected in series, are fabricated using PGREEN rather than P3HT as an active layer. Interestingly, the V_{oc} measured under controlled A.M. 1.5 illumination is significantly lower than that measured with a voltmeter in outdoor conditions in midday sunshine. This is most likely due to the outdoor light intensity

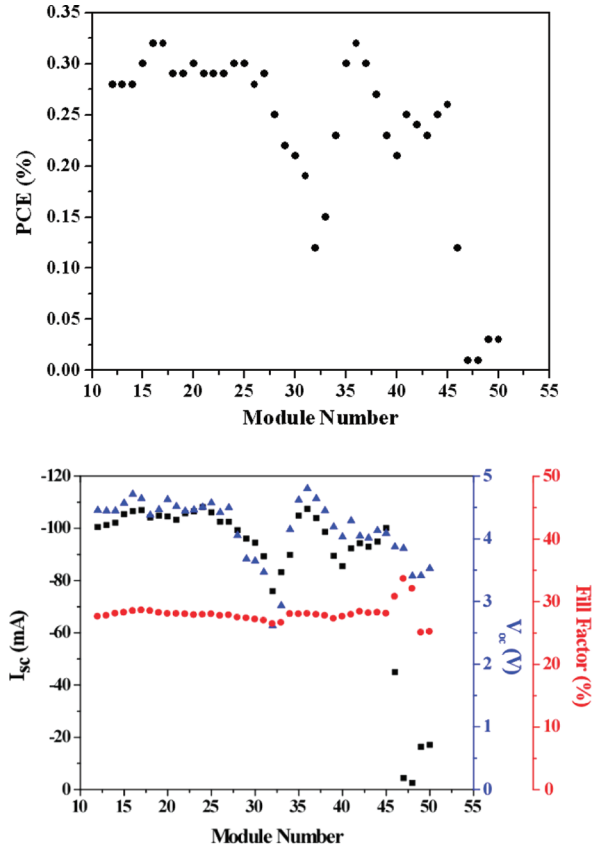

Figure 6. (a) PCE evaluation of slot-die-printed modules. The active area of the modules was 450 cm^2. (b) Short circuit current (I_{sc}), open circuit voltage (V_{oc}), and fill factor (%) of the slot-die-printed modules.

being greater than A.M. 1.5, as it has been shown that increasing light intensity increases V_{oc}.[46]

4. CONCLUSION

In this study, we demonstrate one of the first scale-ups of polymer solar cells from spin-coated laboratory cells to roll-to-roll printed large area cells that does not utilize P3HT:PCBM as an active layer. Indeed, reproducible syntheses are of critical importance as slight differences in material composition can have drastic effects on performance. Considering device fabrication, as the area of spin-coated laboratory cells increases, the PCE decreases as a result of higher resistance across the device, especially in modules where many devices are connected in series. We also show that there can be drastic differences in the composition of the optimal active layer between thiner spin-coated films and necessarily thicker films fabricated by slot-die coating. Using optimized printing techniques, we exhibit large area prototype solar cells that were blue-green in color and gave up to 0.3% PCE. Finally, we highlight the need for higher conductivity electrodes and contacts in printed solar cells, as well as high mobility active layers, as significant losses due to series resistance occur when increasing device area to dimensions necessary to harvest useful amounts of power from OPVs.

AUTHOR INFORMATION

Corresponding Author

*E-mail: frkr@risoe.dtu.dk (F.C.K.); fso@mse.ufl.edu (F.S.); reynolds@chemistry.gatech.edu (J.R.R.).

Notes

J.R.R. and F.S. have a limited financial interest in Sestar, LLC.

■ ACKNOWLEDGMENTS

This work was supported by SESTAR LLC, the Office of Naval Research (N-00014-11-1-0245), the Danish Strategic Research Council (DSF 2104-05-0052 and 2104-07-0022), and EUDP (j. nr. 64009-0050).

■ REFERENCES

(1) Beaujuge, P. M.; Amb, C. M.; Reynolds, J. R. *Acc. Chem. Res.* **2010**, *43*, 1396.
(2) Hoth, C. N.; Schilinsky, P.; Choulis, S. A.; Brabec, C. J. *Nano Lett.* **2008**, *8*, 2806.
(3) Aernouts, T.; Aleksandrov, T.; Girotto, C.; Genoe, J.; Poortmans, J. *Appl. Phys. Lett.* **2008**, *92*, 033306−3.
(4) Ding, J. M.; de la Fuente Vornbrock, A.; Ting, C.; Subramanian, V. *Sol. Energy Mater. Sol. Cells* **2009**, *93*, 459.
(5) Hoth, C. N.; Choulis, S. A.; Schilinsky, P.; Brabec, C. J. *Adv. Mater.* **2007**, *19*, 3973.
(6) Yu, G.; Gao, J.; Hummelen, J. C.; Wudl, F.; Heeger, A. J. *Science* **1995**, *270*, 1789.
(7) Brabec, C. J.; Gowrisanker, S.; Halls, J. J. M.; Laird, D.; Jia, S.; Williams, S. P. *Adv. Mater.* **2010**, *22*, 3839.
(8) Schilinsky, P.; Waldauf, C.; Brabec, C. J. *Appl. Phys. Lett.* **2002**, *81*, 3885.
(9) Zhao, G.; He, Y.; Li, Y. *Adv. Mater.* **2010**, *22*, 4355.
(10) Steckler, T. T.; Zhang, X.; Hwang, J.; Honeyager, R.; Ohira, S.; Zhang, X.-H.; Grant, A.; Ellinger, S.; Odom, S. A.; Sweat, D.; Tanner, D. B.; Rinzler, A. G.; Barlow, S.; Bredas, J.-L.; Kippelen, B.; Marder, S. R.; Reynolds, J. R. *J. Am. Chem. Soc.* **2009**, *131*, 2824.
(11) Liang, Y.; Yu, L. *Acc. Chem. Res.* **2010**, *43*, 1227.
(12) Liang, Y.; Xu, Z.; Xia, J.; Tsai, S.-T.; Wu, Y.; Li, G.; Ray, C.; Yu, L. *Adv. Mater.* **2010**, *22*, E135.
(13) Park, S. H.; Roy, A.; Beaupre, S.; Cho, S.; Coates, N.; Moon, J. S.; Moses, D.; Leclerc, M.; Lee, K.; Heeger, A. J. *Nat. Photon.* **2009**, *3*, 297.
(14) Wang, E.; Wang, L.; Lan, L.; Luo, C.; Zhuang, W.; Peng, J.; Cao, Y. *Appl. Phys. Lett.* **2008**, *92*, 033307.
(15) Scharber, M. C.; Koppe, M.; Gao, J.; Cordella, F.; Loi, M. A.; Denk, P.; Morana, M.; Egelhaaf, H.-J.; Forberich, K.; Dennler, G.; Gaudiana, R.; Waller, D.; Zhu, Z.; Shi, X.; Brabec, C. J. *Adv. Mater.* **2010**, *22*, 367.
(16) Hou, J.; Chen, H.-Y.; Zhang, S.; Li, G.; Yang, Y. *J. Am. Chem. Soc.* **2008**, *130*, 16144.
(17) Coffin, R. C.; Peet, J.; Rogers, J.; Bazan, G. C. *Nat. Chem.* **2009**, *1*, 657.
(18) Tong, M.; Cho, S.; Rogers, J. T.; Schmidt, K.; Hsu, B. B. Y.; Moses, D.; Coffin, R. C.; Kramer, E. J.; Bazan, G. C.; Heeger, A. J. *Adv. Funct. Mater.* **2010**, *20*, 3959.
(19) Beaujuge, P. M.; Ellinger, S.; Reynolds, J. R. *Nat. Mater.* **2008**, *7*, 795.
(20) Amb, C. M.; Beaujuge, P. M.; Reynolds, J. R. *Adv. Mater.* **2010**, *22*, 724.
(21) Beaujuge, P. M.; Vasilyeva, S. V.; Ellinger, S.; McCarley, T. D.; Reynolds, J. R. *Macromolecules* **2009**, *42*, 3694.
(22) Zhang, F.; Mammo, W.; Andersson, L. M.; Admassie, S.; Andersson, M. R.; Inganäs, O. *Adv. Mater.* **2006**, *18*, 2169.
(23) Beaujuge, P. M.; Subbiah, J.; Choudhury, K. R.; Ellinger, S.; McCarley, T. D.; So, F.; Reynolds, J. R. *Chem. Mater.* **2010**, *22*, 2093.
(24) Subbiah, J.; Beaujuge, P. M.; Choudhury, K. R.; Ellinger, S.; Reynolds, J. R.; So, F. *ACS Appl. Mater. Interfaces* **2009**, *1*, 1154.
(25) Xue, J.; So, F.; Schanze, K. S.; Reynolds, J. R.; PCT Int. Appl. WO 2009070706, 2009.
(26) Helgesen, M.; Sondergaard, R.; Krebs, F. C. *J. Mater. Chem.* **2010**, *20*, 36.
(27) Hadipour, A.; deBoer, B.; Blom, P. W. M. *Adv. Funct. Mater.* **2008**, *18*, 169.
(28) Hau, S. K.; Yip, H.-L.; Jen, A. K. Y. *Polym. Rev.* **2010**, *50*, 474.
(29) Dennler, G.; Scharber, M. C.; Brabec, C. J. *Adv. Mater.* **2009**, *21*, 1323.
(30) Norrman, K.; Madsen, M. V.; Gevorgyan, S. A.; Krebs, F. C. *J. Am. Chem. Soc.* **2010**, *132*, 16883.
(31) Chen, L.-M.; Hong, Z.; Li, G.; Yang, Y. *Adv. Mater.* **2009**, *21*, 1434.
(32) Krebs, F. C. *Sol. Energy. Mater. Sol. Cell* **2009**, *93*, 394.
(33) Krebs, F. C.; Gevorgyan, S. A.; Alstrup, J. *J. Mater. Chem.* **2009**, *19*, 5442.
(34) Krebs, F. C.; Tromholt, T.; Jorgensen, M. *Nanoscale* **2010**, *2*, 873.
(35) Krebs, F. C.; Fyenbo, J.; Jorgensen, M. *J. Mater. Chem.* **2010**, *20*, 8994.
(36) Jeong, W.-I.; Lee, J.; Park, S.-Y.; Kang, J.-W.; Kim, J.-J. *Adv. Funct. Mater.* **2011**, *21*, 343.
(37) Servaites, J. D.; Yeganeh, S.; Marks, T. J.; Ratner, M. A. *Adv. Funct. Mater.* **2010**, *20*, 97.
(38) Voorhies, J. D.; Schurdak, E. J. *Anal. Chem.* **1962**, *34*, 939.
(39) Kline, R. J.; McGehee, M. D.; Kadnikova, E. N.; Liu, J.; Frechet, J. M. J.; Toney, M. F. *Macromolecules* **2005**, *38*, 3312.
(40) Campoy-Quiles, M.; Ferenczi, T.; Agostinelli, T.; Etchegoin, P. G.; Kim, Y.; Anthopoulos, T. D.; Stavrinou, P. N.; Bradley, D. D. C.; Nelson, J. *Nat. Mater.* **2008**, *7*, 158.
(41) Subbiah, J.; Amb, C. M.; Reynolds, J. R.; So, F. *Sol. Energy Mater. Sol. Cells* **2012**, *97*, 97.
(42) Alstrup, J.; Jorgensen, M.; Medford, A. J.; Krebs, F. C. *ACS Appl. Mater. Interfaces* **2010**, *2*, 2819.
(43) Peet, J.; Wen, L.; Byrne, P.; Rodman, S.; Forberich, K.; Shao, Y.; Drolet, N.; Gaudiana, R.; Dennler, G.; Waller, D. *Appl. Phys. Lett.* **2011**, *98*, 043301.
(44) Dennler, G. Future Challenges of the Organic Photovoltaic Industry. In *The 9th International Symposium on Functional Pi-Electron Systems*; Atlanta, May 23−28, 2010 ; Georgia Institute of Technology: Atlanta, 2010.
(45) Madsen, M. V.; Sylvester-Hvid, K. O.; Dastmalchi, B.; Hingerl, K.; Norrman, K.; Tromholt, T.; Manceau, M.; Angmo, K.; Krebs, F. C. *J. Phys. Chem. C.* **2011**, *115*, 10817.
(46) Koster, L. J. A.; Mihailetchi, V. D.; Ramaker, R.; Blom, P. W. M. *Appl. Phys. Lett.* **2005**, *86*, 123509.